Polymer 49 (2008) 5095–5104

Contents lists available at ScienceDirect

Polymer

journal homepage: www.elsevier.com/locate/polymer

Rheology of core cross-linked star polymers

Tor Kit Goh, Kristopher D. Coventry, Anton Blencowe, Greg G. Qiao*

Polymer Science Group, Department of Chemical and Biomolecular Engineering, The University of Melbourne, Parkville, Victoria 3010, Australia

ARTICLE INFO

Article history:
Received 14 April 2008
Received in revised form 10 August 2008
Accepted 15 September 2008
Available online 27 September 2008

Keywords:
Rheology
CCS polymer
Molecular softness

ABSTRACT

The rheological characterization for a set of structurally diverse core cross-linked star (CCS) polymers is presented. The influence of arm molecular weight ($M_{w(arm)}$) and CCS polymer molecular weight ($M_{w(CCSP)}$) on the steady- and dynamic-shear properties determined by plate rheometry will be discussed. Both these parameters dramatically affect the CCS polymer solution properties and determine its "molecular softness"; a key feature of star polymers. Data from light scattering and capillary viscometry analysis are also presented to relate the dimensional configuration of the CCS polymers to their rheological properties. The methodology for tuning the structure of the CCS polymer is provided and the implications on solution properties are discussed.

1. Introduction

The ability to design custom polymeric architectures such as densely branched, multi-arm star polymers by living radical polymerization is becoming increasingly routine using existing synthetic techniques [1,2], but the challenge of predicting the influence of these different architectures on the bulk rheology of polymer solutions remains challenging.

To date, the majority of experimental and theoretical data for star polymer dynamics have been studied using anionically polymerized star polymers with a chlorosilane hyperbranched core [3–5] and block copolymer micelles [6,7]. Chlorosilane-core star polymers have low polydispersities (usually ~1.1), a well-defined structure and can be produced in high yield; hence, they make excellent model compounds. A recent review on star polymer behavior was compiled by Vlassopoulos et al. [4] for chlorosilane-core polybutadiene star polymers, where they described the conformity of these star polymers to the Daoud and Cotton model [8] and related an extensive set of characterization data to existing theoretical models and computer simulation data. Others [3,5] have also used these polymers as a basis for understanding star polymer dynamics. Despite extensive use in the literature, widespread applicability of chlorosilane-core star polymers is limited by the anionic polymerization route, which requires stringent reaction conditions, high purity reagents and is limited in its selection of monomers. Block copolymer micelles, on the other hand, overcome some of these limitations especially with regards to monomer selection and can be synthesized by a variety of polymerization methods. The cores may also be cross-linked [7], essentially creating a core cross-linked star (CCS) polymer.

Synthesizing CCS polymers by non-self-assembly methods can also be achieved; the most common method being the "arms-first" synthetic route. This was first reported using anionic polymerization [9] and has been successfully adapted to living radical polymerization, which allows for a broad selection of monomers and less rigorous reaction conditions. The resulting CCS polymers have a dense, cross-linked core (typically 10–30% by mass) with multiple radiating linear arms. Molecular weights are well controlled over a broad range (in this study, up to 5400 kDa) and narrow polydispersities (PDI < 1.4) are achieved with good yields. The star structure is well defined and structural diversity is facilitated by tunable arm and core sizes [2]. It is only through this method and the core cross-linking of micelles that one can obtain a star polymer with a cross-linked core; the former method has been preferred for investigations in honeycomb film fabrication, polymer-supported catalysts, drug delivery and others [10], undoubtedly because it offers incomparable benefits in synthesis and polymer structure. To date, the rheological characterization of CCS polymers synthesized *via* living radical polymerization has not been reported; an independent study of their rheological properties is thus required. In the following study, characterization by light scattering and capillary viscometry were used to determine the dimensional configuration of the CCS polymers. Experimental results from plate rheometry analysis of solutions of CCS polymers by steady and dynamic shear were subsequently related to their macromolecular architecture.

* Corresponding author. Tel.: +61 3 8344 8665; fax: +61 3 8344 4153.
E-mail address: gregghq@unimelb.edu.au (G.G. Qiao).

0032-3861/$ – see front matter © 2008 Elsevier Ltd. All rights reserved.
doi:10.1016/j.polymer.2008.09.030

2. Experimental section

2.1. Materials

Methyl methacrylate (MMA, 99%+) and ethylene glycol dimethacrylate (EGDMA, 98%) were purchased from Aldrich and purified by passing through a column of basic alumina and inhibitor remover (Aldrich). *p*-Toluenesulfonyl chloride (TsCl, 99%+), copper(I) chloride (97%), 2,2′-bipyridine (bpy, 99%+), diethyl phthalate (DEP, 99.5%) and anhydrous anisole (99.7%) were purchased from Aldrich and used without further purification. Toluene, methanol and tetrahydrofuran (THF) were obtained from British Drug Houses (BDH) Ltd. and used without further purification. PMMA–PEGDMA CCS polymers were prepared using previously established methods [1] and the detailed synthetic description is available in the Supplementary information.

2.2. Characterization

Gel permeation chromatography (GPC) was performed on a system fitted with a Wyatt DAWN EOS multi-angle laser light scattering (MALLS) detector ($\lambda = 690$ nm, 30 mW), a Wyatt OPTILAB DSP interferometric refractometer ($\lambda = 690$ nm) and a Shimadzu SPD-10A UV–vis detector using three Phenomenex phenogel columns (porosities of 500, 10^4 and 10^6 Å) and GPC-grade THF (conducted at 30 °C and a flow rate of 1 ml min^{-1}). Molecular weights and polydispersities (PDI; M_w/M_n) were calculated using Astra software (Wyatt Technology Corp.) based on a PMMA d*n*/d*c* value of 0.085 [11]. Gas chromatography–mass spectroscopy (GCMS) was performed on a Shimadzu GC-17A gas chromatograph with a Shimadzu GCMS-QP5000 electron ionization mass spectrometer and Zebron ZB-5 capillary column (solid phase 5% phenyl–95% dimethylpolysiloxane, 30 m × 0.25 mm × 0.25 μm). The injection and interface temperatures were 250 and 230 °C, respectively, and the temperature program was as follows: 40–55 °C at 7 °C min^{-1}, 55–235 °C at 10 °C min^{-1}. Dynamic light scattering (DLS) measurements were performed on a Malvern High Performance Particle Sizer (HPPS) with a He–Ne laser (633 nm) at an angle of 173°. All DLS measurements were performed in THF at 25 °C. Intrinsic viscosity measurements were conducted in a dilution-type Ubbelohde viscometer (Type 531 03/0c) with a capillary diameter of 0.46 mm. The viscometer was connected to an automated viscometer setup (Schott Geräte) comprising of an AVS 360 viscosity measuring unit, measurement tripod with optoelectronic sensors, and a TITRONIC® Universal automated titrator. All measurements were conducted in a CT53 thermostated water bath (Schott Geräte) at 25 ± 0.01 °C. The software "Limited Viscosity Number" (version 4.3.31, UG Software, Germany) was used to process the data and obtain the intrinsic viscosities, as follows: Three consecutive readings were obtained for a given concentration, after which the polymeric solution was diluted with THF and the measurements repeated. The Hagenbach correction factor was applied to all measurements and a minimum of four dilutions (1.5–5 g/100 ml) were used in the determination of the intrinsic viscosity. Samples for GPC–MALLS, DLS and intrinsic viscosity measurements were initially filtered through a 45 μm syringe filter. Rheometry was carried out with an Advanced Rheometric Expansion System (ARES) rheometer (TA Instruments) with a recirculating fluid bath stage at 25 ± 0.1 °C. Experiments were carried out using 50 mm parallel plate and cone and plate geometries made from 316 stainless steel and ground to a specification of 16 RMS. Good agreement was achieved between these two geometries. Further details on the rheometric methods can be found in Section 3. The polymers were dried under vacuum (0.05 mm Hg) for 10 h before being dissolving in a DEP–chloroform co-solvent mixtures and the chloroform was subsequently evaporated under ambient conditions for up to 2 weeks until the sample weight had stabilized. The resulting polymer–DEP solutions were clear, viscous

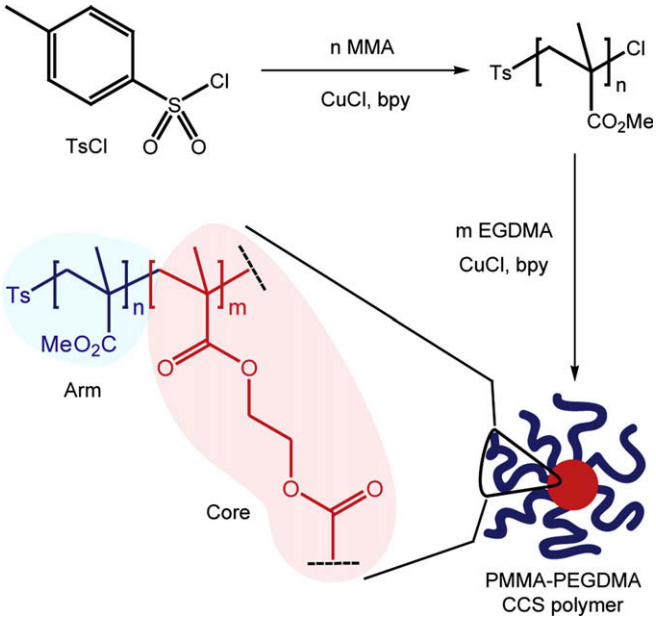

Scheme 1. Synthesis of CCS polymers *via* ATRP was achieved in two-steps; (i) initially, the ATRP initiator TsCl was reacted with MMA to form living PMMA arms, which were isolated and (ii) reacted with EGDMA to form CCS polymers.

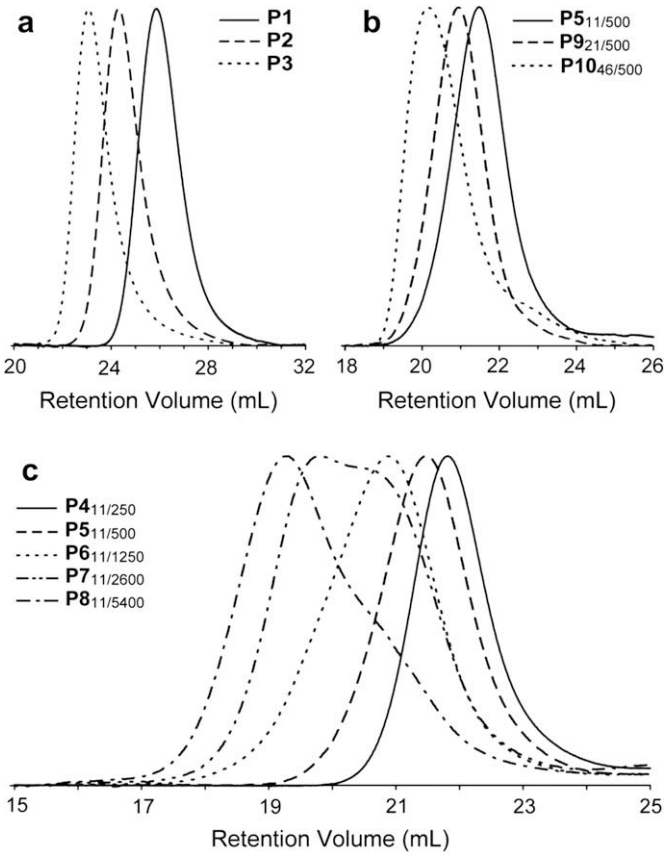

Fig. 1. GPC chromatograms of (**a**) living PMMA arms (**P1**, 11 kDa; **P2**, 21 kDa; **P3**, 46 kDa), (**b**) series of fractionated 500 kDa CCS polymers **P5** and **P9**–**10** with different $M_{w(arm)}$, (**c**) series of fractionated CCS polymers **P4**–**8** with 11 kDa arms and various $M_{w(CCSP)}$.

Table 1
GPC–MALLS data for fractionated CCS polymers **P4**–**10**

Polymer[a]	$M_{w(CCSP)}$[b] (kDa)	PDI[b]	f[c]	$M_{w(arm)}$[b] (kDa)	$M_{w(core)}$[c] (kDa)
P4$_{11/250}$	250	1.08	17	11	51
P5$_{11/500}$	500	1.14	34	11	133
P6$_{11/1250}$	1250	1.23	86	11	299
P7$_{11/2600}$	2600	1.37	180	11	595
P8$_{11/5400}$	5400	1.27	360	11	1250
P9$_{21/500}$	500	1.06	20	21	91
P10$_{46/500}$	500	1.10	10	46	23

[a] The crude polymerization mixture consists of two species of polymer; the CCS polymers and unconverted linear polymer. Fractional precipitation yielded pure CCS polymers.
[b] M_w and PDI (M_w/M_n) were determined by GPC–MALLS.
[c] Number of arms (f) and $M_{w(core)}$ were determined using previously published equations [12].

Table 2
Light scattering and intrinsic viscosity data

Polymer	D_h (nm)[a]	$[\eta]_B$ (dL/g)[b]	g' $[\eta]_B/[\eta]_L$[c]	R_g (nm)[d]
P4$_{11/250}$	11.7	0.21	0.37	8.3
P5$_{11/500}$	16.5	0.22	0.24	9.8
P6$_{11/1250}$	19.6	0.23	0.12	15.2
P7$_{11/2600}$	23.7	0.24	0.08	19.5
P8$_{11/5400}$	26.2	0.35	0.07	27.4
P9$_{21/500}$	16.4	0.34	0.35	12.3
P10$_{46/500}$	21.9	0.48	0.51	15.0

[a] Number-average hydrodynamic radii for polymers dissolved in THF at 25 °C.
[b] Intrinsic viscosities for polymers dissolved in THF at 25 °C.
[c] Intrinsic viscosities of linear polymer $[\eta]_L$ at equivalent M_w to CCS polymers were determined from Eq. (1).
[d] Radius of gyration values determined from GPC–MALLS.

liquids. The concentrations are expressed as $c(\%\ w/w) = (m_{polymer}/(m_{polymer} + m_{DEP})) \times 100$.

3. Results and discussion

3.1. Synthesis of CCS polymers

CCS polymers were prepared by ATRP and the arms-first method (Scheme 1). TsCl was used as an initiator for polymerization of MMA to afford the macroinitiators **P1**–**3** ($M_w = 11$, 21 and 46 kDa, respectively). The macroinitiators were reacted with EGDMA to form PMMA–PEGDMA CCS polymers **P4**–**10**. The f values calculated for each CCS polymer represents the statistical average as the distribution in arm functionality cannot be precisely controlled using this synthetic method.

The polymers are defined by their $M_{w(arm)}$ and $M_{w(CCSP)}$ herein, i.e. **P**$_{11/500}$ is a CCS polymer with 11 kDa arms with an overall M_w of 500 kDa. The star formation step has varying efficiencies in converting the macroinitiators to CCS polymers and therefore, the crude polymerization mixtures contain unconverted low molecular weight material as a by-product. The relative concentration of unconverted species is typically >10%, although it varies with the M_w and concentration of the macroinitiator ($[PMMA\ MI]_0$) used in the star formation reaction and the type of cross-linker employed. The crude CCS polymers were purified *via* fractional precipitation from methanol/THF mixtures. GPC chromatograms of the macroinitiators **P1**–**3** and fractionated CCS polymers **P4**–**10** are presented in Fig. 1, and molecular weight characteristics for these polymers

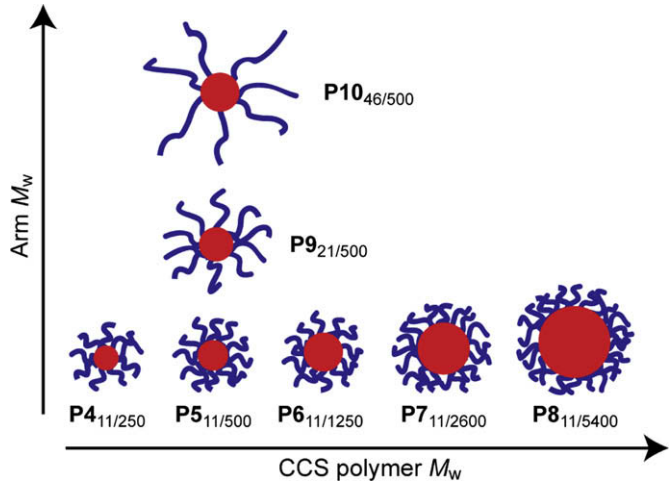

Fig. 2. Pictorial representation of CCS polymers **P4**–**10** with varying $M_{w(CCSP)}$ and $M_{w(arm)}$.

are provided in Table 1. A pictorial representation of the series of CCS polymers used in this study is presented in Fig. 2.

3.2. Characterization of hydrodynamic diameter, radius of gyration and intrinsic viscosity

The CCS polymers used in this rheology study have been characterized for their hydrodynamic diameter (D_h), radius of gyration (R_g) and intrinsic viscosities using dynamic light scattering (DLS), GPC–MALLS and capillary viscometry, respectively (Table 2).

The DLS measurements show a monodisperse size distribution with D_h increasing with $M_{w(CCSP)}$ (Fig. 3a) and $M_{w(arm)}$ (Fig. 3b), respectively. The exception is between **P5**$_{11/500}$ and **P9**$_{21/500}$, which show similar D_h values. Analysis by DLS could have underestimated the D_h value for **P9**$_{21/500}$ due to the decreased branch density at its periphery. The size difference between **P5**$_{11/500}$ and **P9**$_{21/500}$ was observed more distinctly with capillary viscometry and GPC–MALLS analysis.

The intrinsic viscosities of the CCS polymers ($[\eta]_B$), where subscript B denotes star-branched polymers, were determined in THF at 25 °C. For polymers **P4**$_{11/250}$–**P8**$_{11/5400}$, $[\eta]_B$ increased slightly with increasing $M_{w(CCSP)}$. For polymers **P5**$_{11/500}$, **P9**$_{21/500}$ and **P10**$_{46/500}$, increasing $M_{w(arm)}$ caused large increases in $[\eta]_B$. As expected, increasing $M_{w(CCSP)}$ or $M_{w(arm)}$ causes the hydrodynamic volume of the CCS polymer to increase, which leads to an increase in $[\eta]_B$.

The scaling rate of $[\eta]$ with respect to M_w for the CCS polymers is considerably less than linear PMMA and similar to the observed behavior of hyperbranched and dendritic macromolecules [13]. CCS polymers with 11 kDa arms scale with $\alpha = 0.14$ (Fig. 4), which shows the compactness of the star configuration and lack of change in hydrodynamic volume as $M_{w(CCSP)}$ is increased. **P9**$_{21/500}$ and **P10**$_{46/500}$ were omitted from Fig. 4 due to different arm M_ws, however, it is noted that as $M_{w(arm)}$ increases, $[\eta]$ increases rapidly. In Fig. 4, $[\eta]$ for linear PMMA with comparative M_ws were obtained from the Mark–Houwink–Sakurada equation:

$$[\eta] = K \times M_w^{\alpha} \quad (1)$$

The values of $K = 7.5 \times 10^{-3}$ ml/g and $\alpha = 0.72$ obtained from the literature were for living-type PMMA with PDI ≤ 1.25 in THF at 25 °C [14].

To illustrate the effect of f on the hydrodynamic volume of CCS polymers, the branching factor for each of the polymers were determined using the following equation:

$$g' = [\eta]_B/[\eta]_L \quad (2)$$

where g' is the hydrodynamic branching factor, based on $[\eta]$ (subscripts B and L denote star branched and linear polymer, respectively). Linear PMMA $[\eta]_L$ of comparable M_w to the CCS

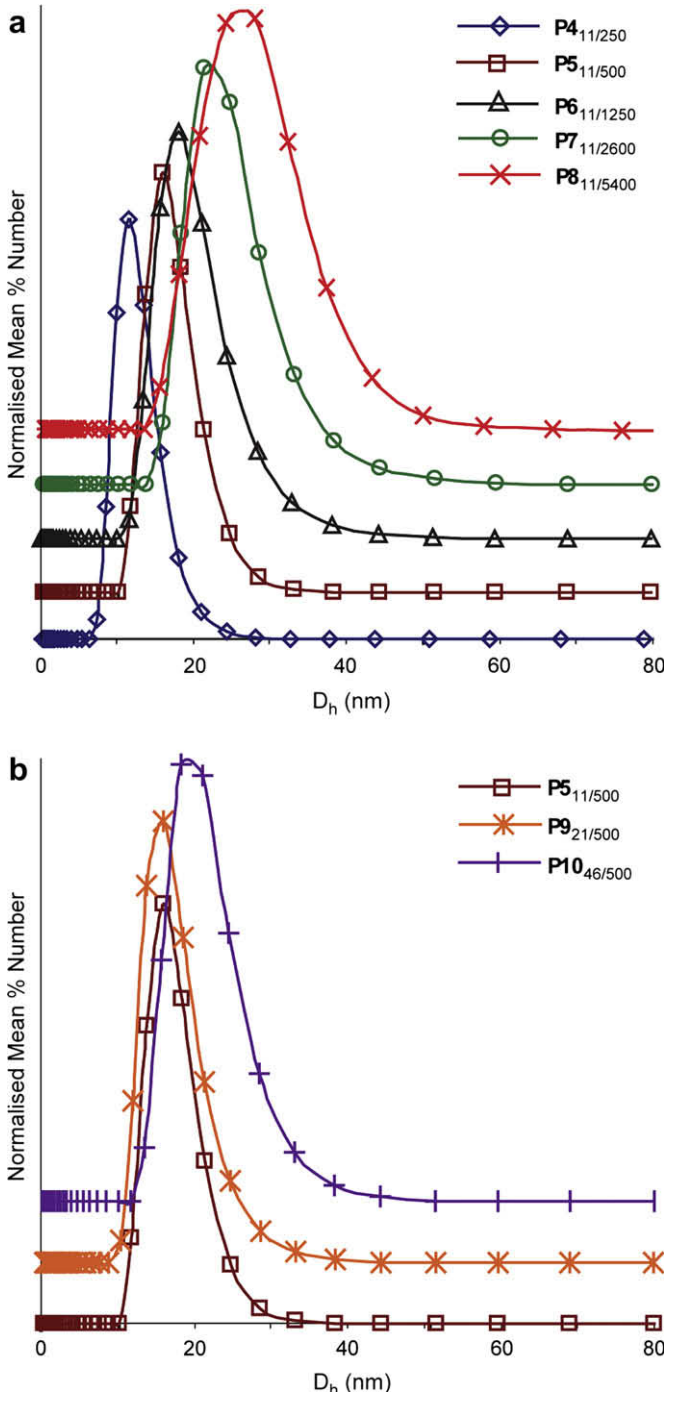

Fig. 3. (**a**) Number-average D_h for CCS polymers **P4–8** with 11 kDa arms and varying $M_{w(CCSP)}$. (**b**) Number-average D_h for 500 kDa CCS polymers **P5** and **P9–10** with varying $M_{w(arm)}$.

polymers were determined from Eq. (1). For CCS polymers with 11 kDa arms and increasing $M_{w(CCSP)}$, it was observed that g' decreases from 0.37 to 0.07. Additionally, 500 kDa CCS polymers with increasing $M_{w(arm)}$ had g' increasing from 0.24 to 0.51. Theoretical predictions [15] and reported data [16,17] on star polymers have shown that g' is solely dependant of f. Thus, Fig. 5 has been compiled to show the effect of f on g' for the CCS polymers. The rapid decrease in g' shows that f greatly affects the viscosity of the polymeric solution due to the tuning of the structure into a more compact configuration.

The seminal work of Daoud and Cotton [8] has been widely cited as the predictive model for scaling behavior of star polymers in

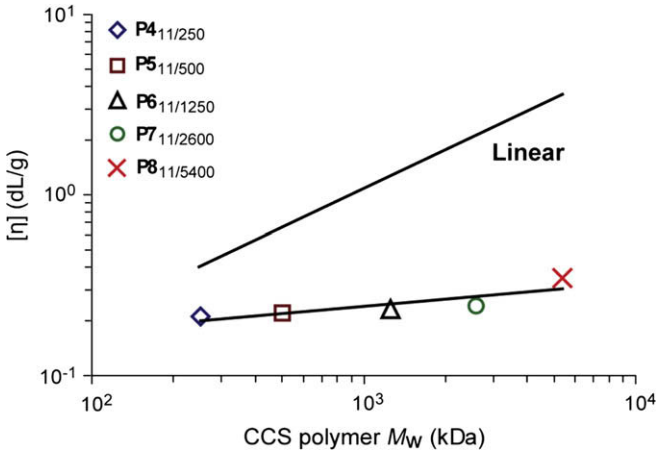

Fig. 4. $M_{w(CCSP)}$ of **P4–8** with 11 kDa arms are plotted versus [η] and compared to linear PMMA [η] as determined from the Mark–Houwink–Sakurada equation. Note that the different M_w CCS polymers have different branching factors (g').

dilute and concentrated solutions, as well as in the melted state. Thus, R_g data from the CCS polymers were applied to the Daoud and Cotton model and their conformity was tested against the scaling relationship:

$$R_g \sim f^{\frac{1}{5}} M_a^{\frac{3}{5}} \tag{3}$$

If only CCS polymers with $f > 20$ are considered (**P5–8**), a reasonably good agreement with Eq. (3) was indeed observed despite these polymers having significant core sizes. However, if all of the CCS polymers (**P4–10**) are considered, divergence from the model is observed and instead scale approximately as $R_g \sim f^{0.47} M_a^{0.68}$. The imposition of the criterion, $f > 20$ was based on the investigations of Gast and coworkers [6], who have observed that moderate aggregation numbers (i.e. f) and long coronal blocks (i.e. long arms relative to the core) are necessary for their star-like model (based on the Daoud and Cotton model) to accurately predict block copolymer micelle scaling behavior. This is required to achieve semi-dilute conditions within the inner-corona of the star and random coil configuration at the outer-corona, respectively. In fact, it was predicted that $f > 17$ was the minimum aggregation number required for micelles to achieve agreement with the star-like model. The arm conformation in the corona of the CCS polymer therefore closely resembles that of star polymers with a molecular core and micelles, which potentially implies that their rheological characteristics and scaling behavior are equally analogous.

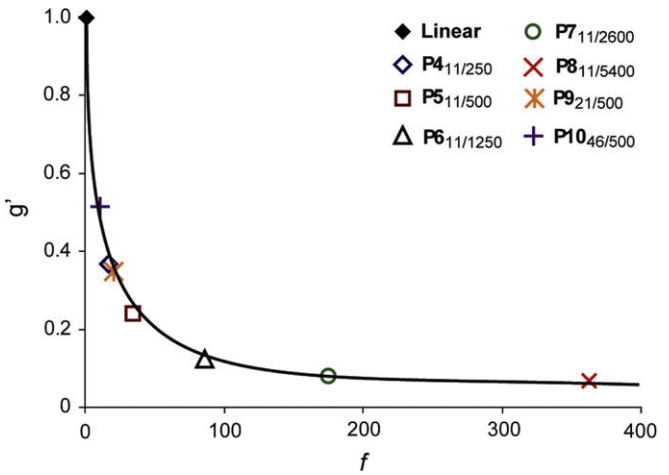

Fig. 5. The hydrodynamic branching factor (g') for all CCS polymers plotted as a function of number of arms (f). Linear polymer has a theoretical g' of 1.

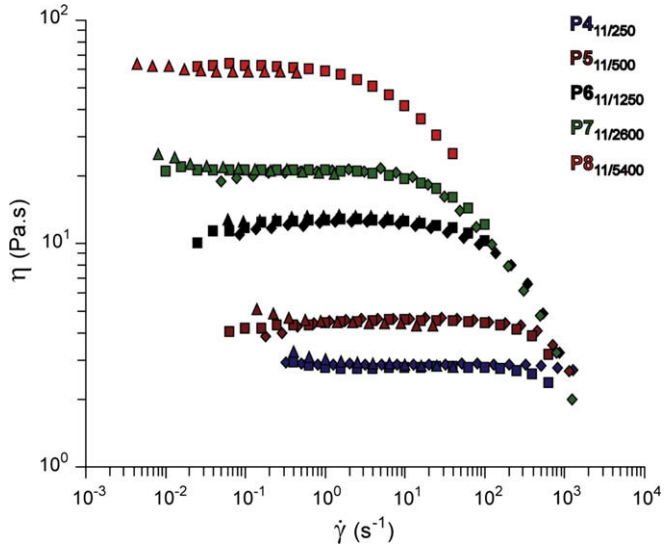

Fig. 6. Steady-shear viscosity profiles for CCS polymers **P4**–**8** with 11 kDa arms and varying $M_{w(CCSP)}$. Data at different % w/w concentrations (10%, ▲; 20%, ■; 30%, ◆) have been shifted to a reference concentration of 20% w/w [17]. The solvent used was DEP and all measurements were recorded at 25 ± 0.1 °C. The top series to the bottom series corresponds to **P8**, **P7**, **P6**, **P5** and **P4**, respectively.

3.3. Rheological characterization

The rheological behavior of CCS polymers was investigated with respect to their macromolecular architecture ($M_{w(arm)}$ and $M_{w(CCSP)}$). Rheological measurements were performed on a controlled strain Advanced Rheometric Expansion System (ARES) using both parallel plate and cone and plate geometries. While the cone and plate geometry has the advantage of a more precisely defined shear rate, parallel plate measurements are in many cases more practical (particularly for high viscosity samples) as it is easier to load the sample and ensures good contact between the rheometer plate surfaces and the polymeric fluid. A sample of comparisons between cone and plate and parallel plate results is provided in the Supplementary information and good agreements of data were observed (S3c–d). Also, slip can be a common cause of errors in rheological measurements of polymer solutions [18] so several samples were analyzed for slip using different gap heights and geometries. In all cases, good agreement was observed and it was concluded that slip was not occurring in the measured range of shear (10^{-2}–10^{2} s^{-1}) and strain (10^{-2}–10^{2}%). All dynamic results reported herein are in the linear viscoelastic region, as determined by dynamic tests over a range of strain amplitudes. Most polymer solutions showed a linear response up to strains of greater than 100%, and some representative strain sweeps are provided in the Supplementary information (S2). All steady-shear viscosity data are at steady state; tests at low shear rates were performed measuring the apparent viscosity as a function of time to ensure that steady state viscosity had been achieved. Repeat experiments revealed a standard deviation of ± 1%. Most samples achieved steady state viscosity in less than 10 s, even at very low shear rates. A representative plot of viscosity versus time is provided in the Supplementary information (S4).

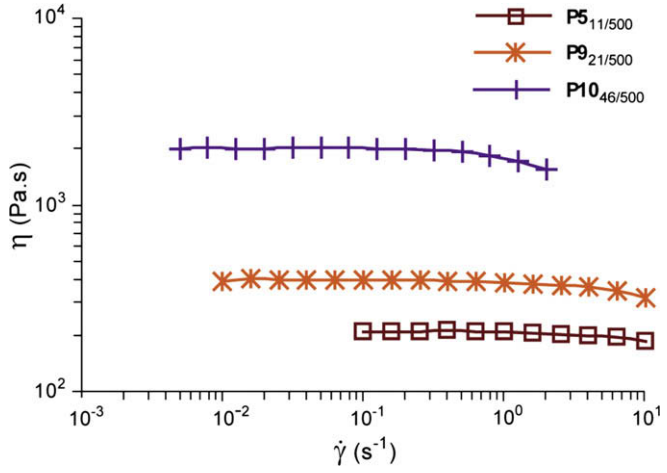

Fig. 7. Steady-shear viscosity profiles for 30% w/w solutions of 500 kDa CCS polymers **P5**$_{11/500}$, **P9**$_{21/500}$ and **P10**$_{46/500}$ with varying $M_{w(arm)}$. The solvent used was DEP and all measurements were recorded at 25 ± 0.1 °C.

3.3.1. Steady-shear characteristics

The shear rate dependencies of solutions of CCS polymers **P4**–**8** with 11 kDa arms are compiled in Fig. 6. Using the method of reduced variables [19], master curves for these polymers were obtained with a reference concentration of 20% w/w. Most solutions showed some shear thinning behavior at the highest shear rates, with the exception of **P4**$_{11/250}$ where no shear thinning was observed up to the maximum obtainable shear rate. However, the

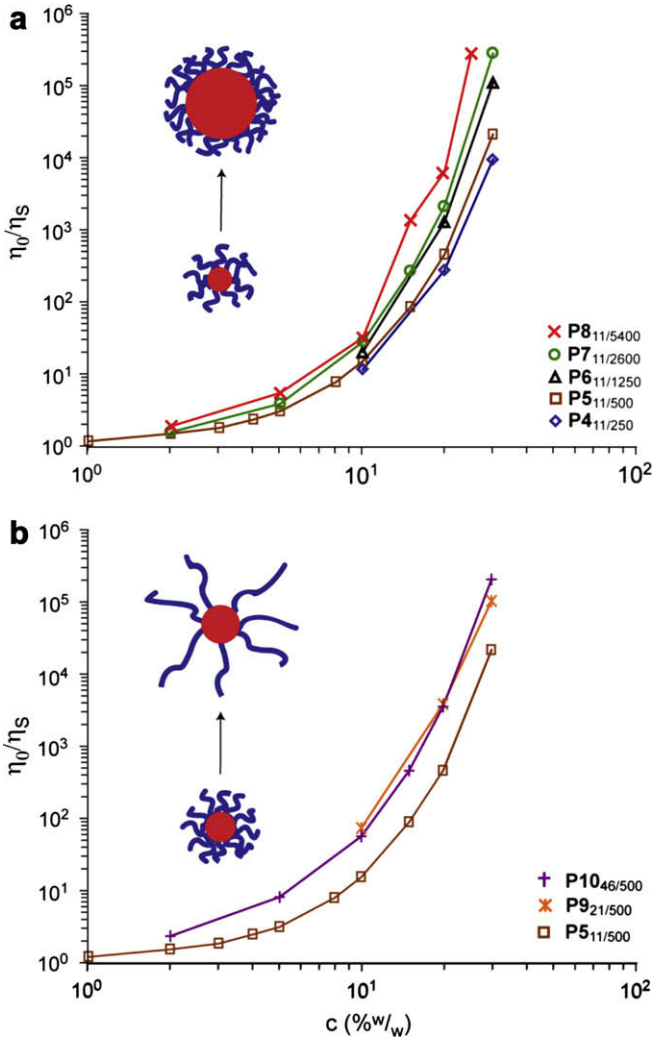

Fig. 8. The relative viscosity (η_0/η_s) as a function of concentration (% w/w) for CCS polymer solutions; (a) **P4**$_{11/250}$–**P8**$_{11/5400}$ with constant $M_{w(arm)}$ and (b) **P5**$_{11/500}$, **P9**$_{21/500}$ and **P10**$_{46/500}$ with constant $M_{w(CCSP)}$. Enhancement of viscosity was observed when either parameter was increased. The solvent used was DEP and all measurements were recorded at 25 ± 0.1 °C. Repeat experiments revealed a standard deviation of ± 1%.

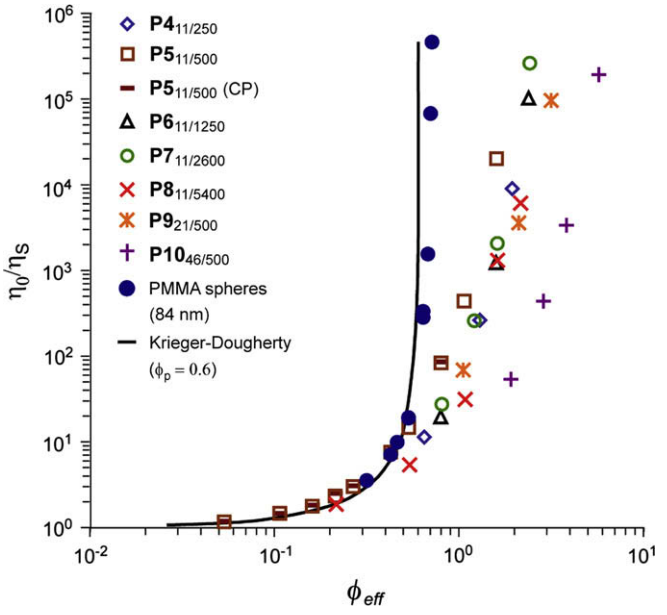

Fig. 9. The relative viscosities (η_0/η_s) for CCS polymer solutions as a function of the effective volume fraction (ϕ_{eff}). The solvent used was DEP and all measurements were recorded at 25 ± 0.1 °C. Data for PMMA hard spheres were obtained from Mewis et al. [22]. The Krieger–Dougherty equation ($\phi_p = 0.6$) is also shown. Repeat experiments revealed a standard deviation of ± 1%.

onset of shear thinning behavior differed for each polymer solution. If we define the characteristic shear rate, $\overline{\gamma}_0$, as the shear rate where the viscosity is reduced to 80% of its zero-shear viscosity (η_0), then it is generally observed that $\overline{\gamma}_0$ decreases as $M_{w(CCSP)}$ is increased.

The shear rate dependencies of 500 kDa CCS polymers **P5**$_{11/500}$, **P9**$_{21/500}$ and **P10**$_{46/500}$ with varying $M_{w(arm)}$ are provided in Fig. 7, where the shear profiles for 30% w/w solutions of the polymer are presented. Unlike the previous 11 kDa arm series (Fig. 6), master curves were not obtained because the polymer solutions at 10 and 20% w/w concentration were Newtonian in nature; viscosities were constant throughout the measured shear rates. Only at concentrations of 30% w/w do **P9**$_{21/500}$ and **P10**$_{46/500}$ show slight shear thinning behavior. Data could not be obtained at higher shear rates due to sample expulsion occurring at $\overline{\gamma} > 10\ s^{-1}$.

The viscosity data for CCS polymer solutions are presented as a plot of the relative viscosity (η_0/η_s, where η_s is the solvent viscosity) as a function of the solution concentration, c(% w/w). For clarity, two plots are provided; Fig. 8a illustrates data for CCS polymers with increasing $M_{w(CCSP)}$ and constant $M_{w(arm)}$ and Fig. 8b illustrates data for CCS polymers with increasing $M_{w(arm)}$ and constant $M_{w(CCSP)}$. For polymers **P4**–**8** the relative viscosities are relatively similar at low concentrations but begin to diverge at $c > 1$% w/w (Fig. 8a). The order of increasing relative viscosities is from the lowest (**P4**) to highest (**P8**) M_w star polymers. Additionally, **P4**$_{11/250}$ shows the least concentration dependence and **P8**$_{11/5400}$ the most. Therefore, despite $M_{w(arm)}$ being equal, the relative viscosities appear to be determined by either $M_{w(CCSP)}$ or f. Vlassopoulos et al. [20] and Likos et al. [21] have shown that it is the latter that controls the viscosity and interaction potential. However, in this study both f and $M_{w(core)}$ are variable; viscosity enhancement as observed in Fig. 8a could possibly be caused by either because both these factors affect the hydrodynamic volume of the star polymer.

For polymers **P5**$_{11/500}$, **P9**$_{21/500}$ and **P10**$_{46/500}$ the $M_{w(CCSP)}$ is equal and the $M_{w(arm)}$ increases, which consequently leads to a reduction in f (Fig. 8b). In a similar observation in Fig. 8a, the relative viscosity increases as the size of the CCS polymer increases (due to increasing $M_{w(arm)}$ in this case). However, the trend of concentration dependence for **P5**, **P9** and **P10** is qualitatively observed to be similar for $c > 10$% w/w. Furthermore, **P9**$_{21/500}$ and **P10**$_{46/500}$ are indistinguishable at $10 < c < 20$% w/w and only a slight deviation is observed for $c = 30$% w/w (where **P10** has a higher relative viscosity). Under dilute conditions employed for the light scattering study, **P9**$_{21/500}$ ($R_g = 12.3$ nm) and **P10**$_{46/500}$ ($R_g = 15.0$ nm) have different radii. However, under semi-dilute conditions the radii of the star polymer changes as the corona is deformed. The **P10**$_{46/500}$ ($f = 10$) corona is more easily deformed due to high f and $M_{w(arm)}$ compared with **P9**$_{21/500}$ ($f = 20$), thus exhibiting viscosity and concentration-dependant behavior which suggests that they have apparently similar conformations.

Plotting the relative viscosity data as a function of the effective volume fraction, which normalizes the CCS polymer sizes [20], allows for analysis purely based on $M_{w(arm)}$, $M_{w(CCSP)}$ and f. Fig. 9 shows the relative viscosity data as a function of the effective volume fraction ($\phi_{eff} = c/c_e$), where the overlap concentrations (c_e)

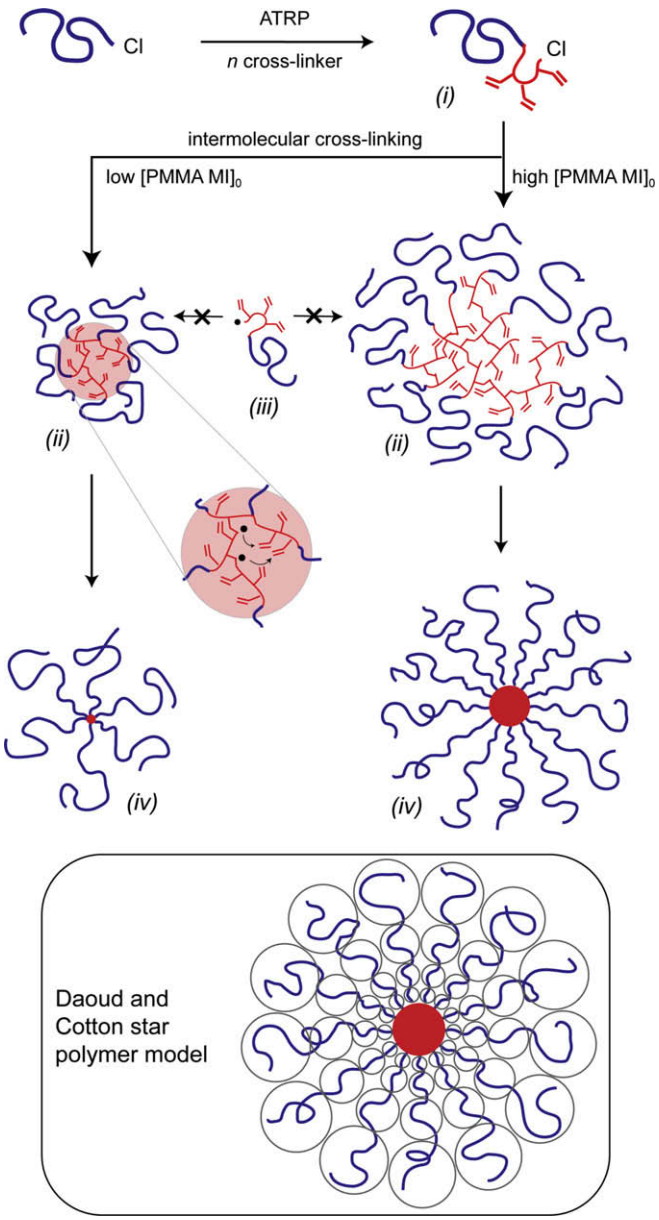

Scheme 2. The proposed mechanism for CCS polymer formation. Macroinitiator concentration ([PMMA MI]$_0$) determines f but the branch density of the loose-core intermediate (*ii*) and subsequently, the CCS polymer (*v*) is comparable for equivalent $M_{w(arm)}$. An elaborate reaction scheme is shown for the low [PMMA MI]$_0$ case. *Inset*: The theoretical Daoud and Cotton star polymer model.

were calculated from DLS analysis. For comparison, data for 84 nm PMMA hard spheres (with a shell of poly(12-hydroxystearic acid), 5 repeat units) in decalin [22] and the Krieger–Dougherty equation (Eq. (4)) for colloidal particles [23,24] are also shown (Fig. 9);

$$\eta_r = \left[1 - \phi/\phi_p\right]^{-[\eta]\phi_p} \quad (4)$$

where η_r is the relative viscosity (η_0/η_s), ϕ is the volume fraction, ϕ_p is the volume fraction of hard spheres at close-packing and $[\eta]$ is the intrinsic viscosity scale factor for Brownian particles as predicted by Einstein [25].

While the Krieger–Dougherty equation predicts the behavior of dilute and non-dilute PMMA hard sphere solutions, deviation in the observed data for the CCS polymers occurs as the polymer solutions become non-dilute ($0.1 < \phi_{eff} < 1$). This is because CCS polymers (as well as other star polymers and micelles) display a "molecular softness" characteristic [3,4,20]; interpenetration and deformation of the "soft" corona leads to deviation from hard sphere behavior as the concentration reaches and surpasses c_e. Whereas PMMA hard spheres achieve close-packing at $\phi < 0.6$, CCS polymers achieve close-packing at significantly higher ϕ values (Fig. 9).

The degree of molecular softness and interaction potential depends on the segmental density of the corona where the radiating linear arms reside. For chlorosilane-core star polymers, this has been observed to be most strongly controlled by f [20]. In this study however, the star polymers have a significantly sized core which adds a degree of complexity to their behavior, as discussed previously (Fig. 8). Polymers **P4**–**8** have equal $M_{w(arm)}$, but increasing f (17–360) and $M_{w(core)}$ (51–1250 kDa), although the core contribution towards the overall M_w remains relatively constant (~25% by

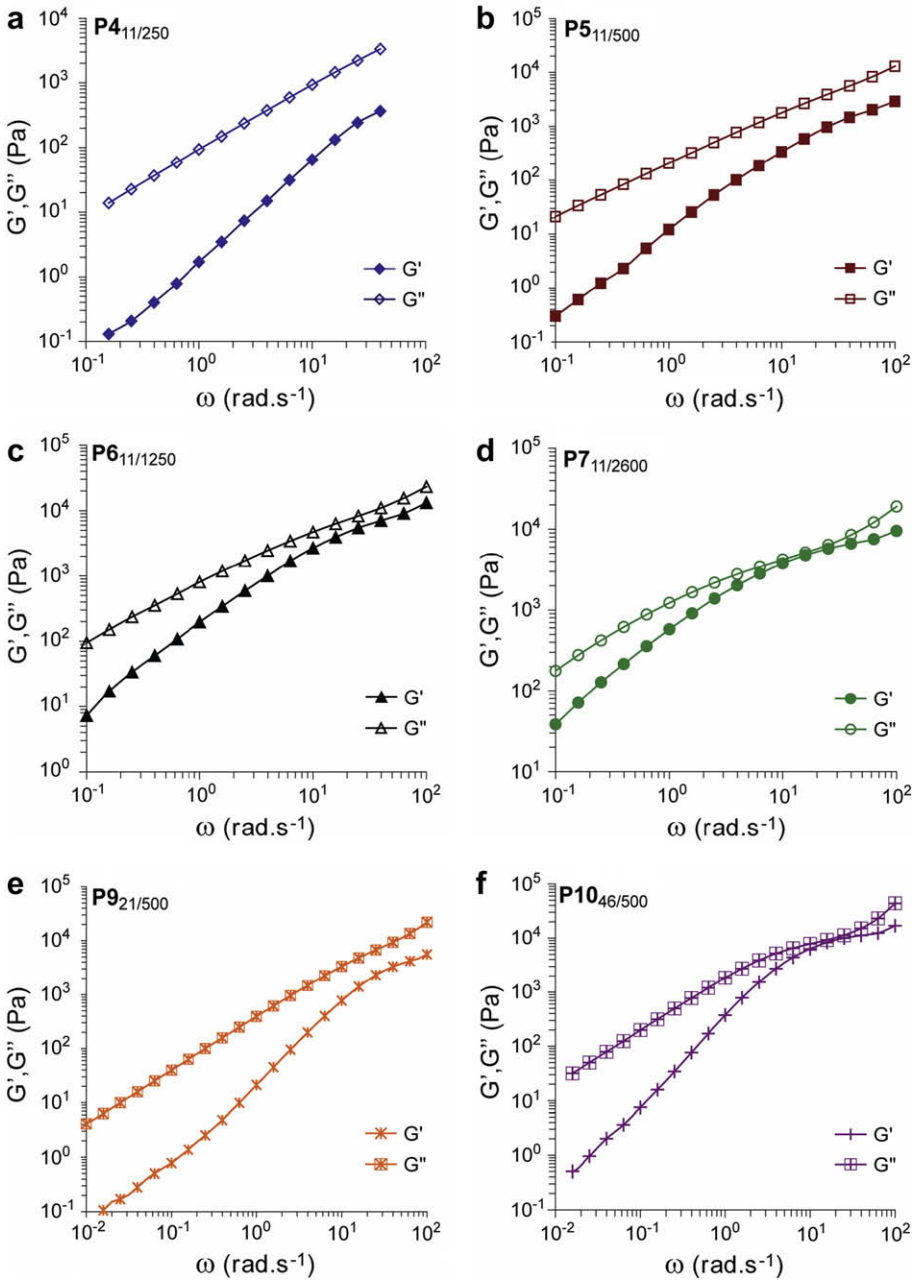

Fig. 10. Storage, G' and loss, G'' moduli for 30% w/w solutions of CCS polymers. (**a**–**d**) CCS polymers **P4**$_{11/250}$–**P7**$_{11/2600}$ with constant $M_{w(arm)}$ and (**b**, **e** and **f**) **P5**$_{11/500}$, **P9**$_{21/500}$ and **P10**$_{46/500}$ with constant $M_{w(CCSP)}$. The solvent used was DEP and all measurements were recorded at 25 ± 0.1 °C.

mass). Their molecular softness however, is nearly indistinguishable within the concentration range tested ($c < 30\%$ w/w). Higher concentration data was not reliable due to sample expulsion. There are two likely explanations; (i) the CCS polymer core itself is deformable and contributes towards the molecular softness together with the radiating linear arms, and core deformability increases (i.e. degree of cross-linking decreases) as f increases, or (ii) the segmental density of the linear polymer corona remains constant because as f increases, so does the core size.

With regards to the former, determination of the degree of cross-linking within the core of CCS polymers prepared via controlled radical polymerization is non-trivial and the authors and others [1,2,10,12] have not been able to determine this parameter quantitatively. However, it should be noted that for cross-linked micelles Liu and coworkers were able to determine the degree of cross-linking to be *ca.* 40% using UV–visible spectroscopy to monitor the photodimerization of cinnamoyl moieties [7b]. Unfortunately, similar spectroscopic methods are inappropriate for the determination of the degree of cross-linking in CCS polymers prepared via controlled radical polymerization as a result of differences in the cross-linking mechanism and overlapping absorptions. However, it is probable that the cores have a high degree of cross-linking due to the high cross-linking efficiencies of the divinyl monomers used. This is supported by evidence from NMR spectra [2b–d,10f] recorded at various times during the CCS polymer formation process. For example, NMR spectra of reaction products obtained at very short reaction times reveal the formation of block prepolymers with resonances being observed for both the cross-linkers central segment and pendant vinyl groups. In comparison, spectra of reaction products recorded at long reaction times reveal very few or no resonances corresponding to vinyl groups, whereas resonances due to the cross-linkers central segment are still visible. Although the reduction of vinyl group resonances could result from the restricted mobility of the core, the observation of resonances resulting from the cross-linkers central segments implies that the majority of vinyl groups have reacted to form cores with high degrees of cross-linking. It is therefore reasonable to assume that the rigidity of the polymer cores is very similar (i.e. the cross-linking density remains constant with increasing f). Hence, it seems more likely that the latter explanation is the probable cause of the similar molecular softness; as f increases and $M_{w(core)}$ increases, the segmental density of the linear polymer corona remains relatively constant.

In comparison, a clear trend can be observed for polymers **P5**$_{11/500}$ ($f = 34$), **P9**$_{21/500}$ ($f = 20$) and **P10**$_{46/500}$ ($f = 10$), in which the $M_{w(arm)}$ increases whilst the $M_{w(CCSP)}$ remains constant (Fig. 9). As the linear arms increase in size, the star polymer becomes softer as the thickness of the deformable corona increases and the segmental density decreases. For this set of polymers, decreasing f further increases the softness and therefore, high volume fractions are achievable.

3.3.2. Relationship between CCS polymer molecular softness and polymerization mechanism

It is proposed that the comparable molecular softness observed for CCS polymers **P4**$_{11/250}$–**P8**$_{11/5400}$ is related to the nature of the arms-first synthetic approach (Scheme 2). During the initial stage of the reaction, PMMA–PEGDMA block prepolymers are formed that are predominantly linear [2b–d,10f,26] and possess a random chain conformation (Scheme 2, (*i*)). Subsequently, the block prepolymers react with each other *via* radical attack on the pendant vinyl groups forming intermediate, loosely cross-linked macromolecules (Scheme 2, (*ii*)). The number of block prepolymers that link together (which is directly proportional to f) increases with increasing [PMMA MI]$_0$, but the random coil block prepolymers pack in a radial conformation around the "loose core" to a similar degree. This is because the block size of PEGDMA relative to PMMA (which is controlled by the EGDMA:MI ratio) is similar, therefore increasing f increases core size ($M_{w(core)}$) concurrently. Further intermolecular cross-linking with unreacted block prepolymers (Scheme 2, (*iii*)) is restricted once the intermediate becomes congested and intramolecular cross-linking within the core prevails. The loosely cross-linked intermediate exists for only a short time (relative to the entire synthesis), thus higher segmental densities are not achievable as in the case of linking linear polymers with a molecular core (e.g. chlorosilane-core star polymers, where the exclusive linking reaction and long time scales allow for high branch densities to be achieved). As the PMMA blocks are brought closer together as a result of intramolecular cross-linking, perturbation and chain stretching occurs from the inner-corona outwards. If high branch densities are achieved [27], the PMMA blocks obtain a semi-dilute and random coil conformation at the inner and outer-corona, respectively; i.e. they become star polymer "arms". As the block prepolymer branch density of the loose-core intermediate is

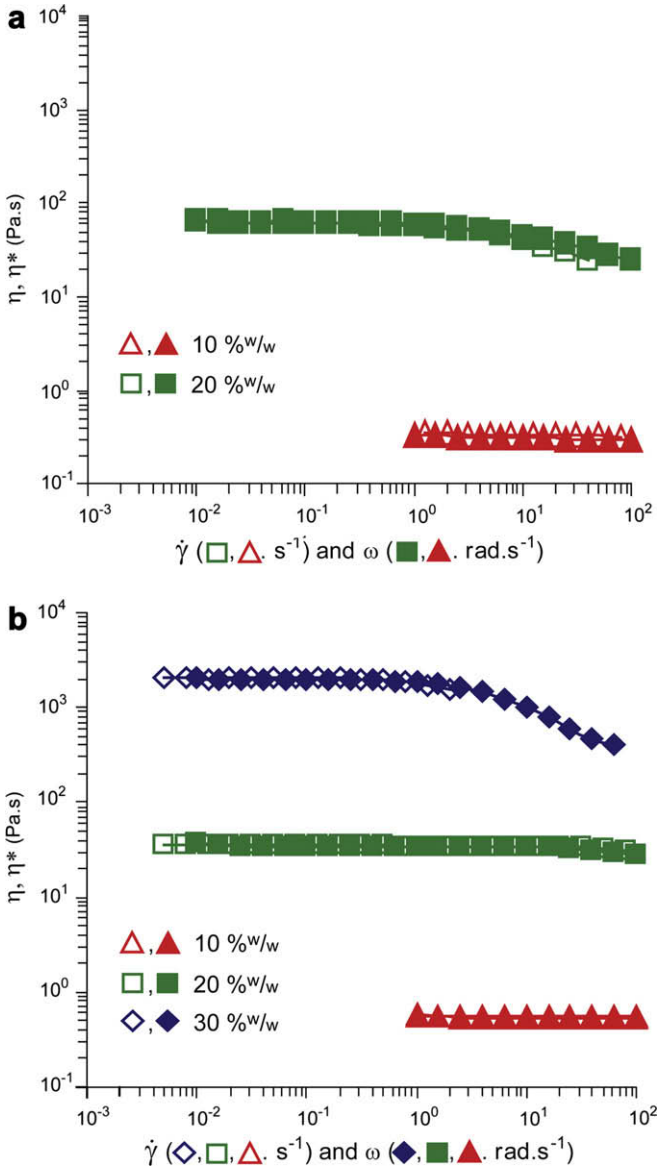

Fig. 11. Plots of shear rate ($\dot{\gamma}$) and angular frequency (ω) versus viscosity for solutions of (**a**) **P8**$_{11/5400}$ and (**b**) **P10**$_{46/500}$. Filled symbols indicate $\eta^*(\omega)$ data and empty symbols indicate $\eta(\dot{\gamma})$ data. Solution w/w concentrations are indicated as follows: 10%, ◇ or ◆; 20%, △ or▲; 30%, □ or ■. The solvent used was DEP and all measurements were recorded at 25 ± 0.1 °C. Repeat experiments revealed a standard deviation of ± 1%.

equal for equivalent $M_{w(arm)}$, the CCS polymer in its final state (Scheme 2, (*iv*)) should also have similar branch densities for equivalent $M_{w(arm)}$ and thus, comparable molecular softness.

3.3.3. Dynamic shear characteristics

The dynamic behavior of solutions of CCS polymers **P4**$_{11/250}$–**P7**$_{11/2600}$ was investigated in terms of the storage (G') and loss (G'') moduli for polymer solutions of 30% w/w concentration (Fig. 10a–d, respectively). It is evident from the G'' profiles that the solutions of CCS polymers changed from Newtonian to viscoelastic behavior with increasing $M_{w(CCSP)}$. This is consistent with steady-shear data where decreasing $\dot{\gamma}_0$ occurs with increasing $M_{w(CCSP)}$. While the elastic contribution to the behavior of the lower $M_{w(CCSP)}$ solutions was substantially less significant than the viscous contribution over the observed range, it was nevertheless measurable and increasing in significance at higher frequencies. It would be interesting to observe the behavior of this material at still higher frequencies, for example using a piezoelastic axial vibrator [28].

A similar transition occurred upon investigation of the dynamic moduli of 500 kDa CCS polymers **P5**$_{11/500}$, **P9**$_{21/500}$ and **P10**$_{46/500}$ in 30% w/w solutions (Fig. 10b, e and f, respectively). The G'' modulus for **P5**$_{11/500}$ indicates that this solution is largely Newtonian in behavior. **P9**$_{21/500}$ showed slight viscoelasticity at high ω, whereas **P10**$_{46/500}$ showed more pronounced viscoelastic behavior. Again, this is consistent with steady-shear data where only slight shear thinning was observed for **P5**$_{11/500}$ and **P9**$_{21/500}$, whereas **P10**$_{46/500}$ showed more pronounced shear thinning behavior. Thus, it is observed that increasing $M_{w(CCSP)}$ or $M_{w(arm)}$ changes the solution behavior from Newtonian to viscoelastic.

The viscosity profiles obtained from dynamic and steady-shear experiments were compared to see if the Cox–Merz rule applied to these polymer solutions. It was observed that all polymer solutions showed excellent agreement between the dynamic and steady-shear viscosity data. Fig. 11 is a typical illustration of such data, with **P8**$_{11/5400}$ and **P10**$_{46/500}$ showing good agreement of $\eta^*(\omega)$ and $\eta(\dot{\gamma})$ data at 10 and 20% w/w concentrations.

4. Conclusion

The rheology of poly(methyl methacrylate)–poly(ethylene glycol dimethacrylate) (PMMA–PEGDMA) core cross-linked star polymers was investigated using a systematic series of polymers with varying $M_{w(arm)}$ (11–46 kDa), $M_{w(CCSP)}$ (250–5400 kDa) and f (10–363). This diverse set of polymers was synthesized *via* ATRP and the arms-first approach. Characterization by dynamic light scattering and capillary viscometry determined that the CCS polymers possessed D_h and g' of 12–26 nm and 0.51–0.07, respectively. Additionally, the observed R_g data indicated that CCS polymers with $f > 20$ conform to Daoud and Cotton model and showed typical star polymer scaling behavior. These macromolecules were dissolved in a good solvent for the polymer (10, 20 and 30% w/w) and subjected to steady and dynamic shear, during which their rheological properties were measured. For constant $M_{w(arm)}$ CCS polymers, an increase in f and $M_{w(CCSP)}$ caused the viscosity and concentration dependence to increase, undoubtedly because the hydrodynamic volume of the CCS polymers was concurrently increased. The viscosity enhancement effect was similarly observed for constant $M_{w(CCSP)}$ CCS polymers, however the concentration dependence was qualitatively similar. Furthermore, plotting of the viscosity data against the effective volume fraction allowed for the observation of molecular softness, a typical characteristic for star-shaped polymers. In a novel observation, constant $M_{w(arm)}$ CCS polymers were observed to have similar molecular softness (despite changing f and $M_{w(CCSP)}$). This phenomenon was related to the arms-first synthetic approach after careful consideration of the polymerization mechanisms. The dynamic behavior was also observed to be affected by the CCS polymer structure, with both $M_{w(arm)}$ and $M_{w(CCSP)}$ determining solution behavior; transition from Newtonian to viscoelastic behavior was clearly observed when both these structural parameters were increased independently. Finally, CCS polymer solutions were found to obey the Cox–Merz rule.

Acknowledgements

The authors thank Peter Scales and Jonathan Foong from the Particulates and Fluids Processing Centre (PFPC) for the use of the ARES rheometer and Robert Shanks from the Department of Applied Sciences, Royal Melbourne Institute of Technology for the use of the automated viscometer. The authors also thank Viyada Tirtaatmadja for critical reading of the manuscript.

Appendix. Supplementary information

Results on polymer–DEP solution stability, characterization with different gap heights and geometries, dynamic strain responses, time-dependant steady-shear data and detailed synthetic procedures for **P1**–**10**. Supplementary information associated with this article can be found in the online version, at doi:10.1016/j.polymer.2008.09.030.

References

[1] (a) Solomon DH, Qiao GG, Abrol S. Process for microgel preparation. WO9958588; 1999;
(b) Baek KY, Kamigaito M, Sawamoto M. Macromolecules 2001;34:215–21;
(c) Baek KY, Kamigaito M, Sawamoto M. J Polym Sci Part A Polym Chem 2002;40:633–41;
(d) Gurr PA, Qiao GG, Solomon DH. Macromolecules 2003;36:5650–4.
[2] (a) Xia JH, Zhang X, Matyjaszewski K. Macromolecules 1999;32:4482–4;
(b) Zhang X, Xia JH, Matyjaszewski K. Macromolecules 2000;33:2340–5;
(c) Baek KY, Kamigaito M, Sawamoto M. Macromolecules 2001;34:7629–35;
(d) Baek KY, Kamigaito M, Sawamoto M. J Polym Sci Part A Polym Chem 2002;40:1972–82;
(e) Gurr PA. The synthesis and characterization of star-microgels by atom transfer radical polymerization. Ph.D. thesis, University of Melbourne, Australia; 2004.
[3] Grest GS, Fetters LJ, Huang JS, Richter D. Adv Chem Phys 1996;XCIV:67–164.
[4] Vlassopoulos D, Fytas G, Pakula T, Roovers J. J Phys Condens Matter 2001;13:R855–76.
[5] Bauer BJ, Fetters LJ, Graessley WW, Hadjichristidis N, Quack GF. Macromolecules 1989;22:2337–47.
[6] (a) Gast AP. Langmuir 1996;12:4060–7;
(b) Cogan KA, Gast AP, Capel M. Macromolecules 1991;24:6512–20.
[7] (a) Loppinet B, Fytas G, Vlassopoulos D, Likos CN, Meier G, Liu GJ. Macromol Chem Phys 2005;206:163–72;
(b) Tao J, Stewart S, Liu GJ, Yang M. Macromolecules 1997;30:2738–45.
[8] Daoud M, Cotton JP. J Phys (Paris) 1982;43:531–8.
[9] Zilliox J-G, Rempp P, Parrod JJ. J Polym Sci Part C 1968;22:145–56.
[10] For honeycomb films: (a) Connal LA, Gurr PA, Qiao GG, Solomon DH. J Mater Chem 2004;15:1286–92;
(b) Connal LA, Qiao GG. Adv Mater 2006;18:3024–8;
(c) Connal LA, Qiao GG. Soft Matter 2007;3:837–9;
For core-functional CCS polymers: (d) Terashima T, Kamigaito M, Baek K-Y, Ando T, Sawamoto M. J Am Chem Soc 2003;125:5288–9;
(e) Helms B, Guillaudeu SJ, Xie Y, McMurdo M, Hawker CJ, Fréchet JMJ. Angew Chem Int Ed 2005;44:6384–7.
(f) Terashima T, Ouchi M, Ando T, Sawamoto M, Kamigaito M. J Polym Sci Part A Polym Chem 2006;44:4966–80.
(g) Terashima T, Ouchi M, Ando T, Kamigaito M, Sawamoto M. Macromolecules 2007;40:3581–8;
(h) Blencowe A, Goh TK, Best S, Qiao GG. Polymer 2008;49:825–30. For drug delivery applications;
(i) Wiltshire J, Qiao GG. Aust J Chem 2007;60:699–705, and references therein. For engine performance lubricants;
(j) Kennedy JP, Jacob S. Acc Chem Res 1998;31:835–41, and references therein.
[11] (a) Michielsen S. Specific refractive index increments of polymers in dilute solutions. In: Brandup J, Immergut EH, Grulke EA, editors. Polymer handbook. 4th ed., vol. 2. Hoboken, NJ: John Wiley and Sons, Inc.; 1999. VII/547;
(b) The dn/dc of densely branched CCS polymers and linear polymers of the same monomeric constitution were reported to be comparable by Gao H, Tsarevsky NV, Matyjaszewski K. Macromolecules 2005;38:5995–6004.
[12] Wiltshire JT, Qiao GG. Macromolecules 2006;39:9018–27.
[13] Mourey TH, Turner SR, Rubinstein M, Fréchet JMJ, Hawker CJ, Wooley KL. Macromolecules 1992;25:2401–6.

[14] Kurata M, Tsunashima Y. Viscosity–molecular weight relationships and unperturbed dimensions of linear chain molecules. In: Brandup J, Immergut EH, Grulke EA, editors. Polymer handbook. 4th ed., vol. 2. Hoboken, NJ: John Wiley and Sons, Inc.; 1999. VII/1.
[15] (a) Zimm BH, Stockmayer WH. J Chem Phys 1949;17(12):1301–14;
(b) Ham JS. J Chem Phys 1957;26(3):625–33.
[16] (a) Kraus G, Gruver JT. J Polym Sci Part A Polym Chem 1965;3(1):105–22;
(b) Graessley WW, Masuda T, Roovers JEL, Hadjichristidis N. Macromolecules 1976;9:127–41;
(c) Graessley WW, Roovers JEL. Macromolecules 1979;12:959–65;
(d) Graessley WW. Acc Chem Res 1977;10:332–9.
[17] (a) Omura N, Kennedy JP. Macromolecules 1997;30:3204–14;
(b) Marsalkó TM, Majoros I, Kennedy JP. J Mater Sci Pure Appl Chem 1997;A34:775–92.
[18] (a) Yoshimura A, Prud'homme RK. J Rheol 1988;32(1):53–67;
(b) Gregory T, Mayers S. JOCCA 1993;2:82–6.
[19] Ferry JD. Viscoelastic properties of polymers. NY: John Wiley and Sons; 1980.
[20] Vlassopoulos D, Fytas G, Pispas S, Hadjichristidis N. Physica B 2001;296:184–9.
[21] Likos CN, Lwen H, Watzlawek M, Abbas B, Jucknischke O, Allgaier J, Richter D. Phys Rev Lett 1998;80(20):4450–3.
[22] Mewis J, Frith WJ, Strivens TA, Russel WB. AIChE J 1989;35(3):415–22.
[23] Krieger IM. Adv Colloid Interface Sci 1972;3:111.
[24] Roovers J. Macromolecules 1994;27:5359–64.
[25] Einstein A. Ann Phys Leipzig 1906;19:371–81.
[26] Terashima T. Multifunctional designer catalysts via living radical polymerization. Ph.D. thesis, Kyoto University, Japan; 2007.
[27] High branch densities are achievable when $f > 17$ and coronal blocks are long compared to the core blocks [see Ref. [6]], such that the star polymer "arms" have a concentration gradient which decays with increasing distance from the core. The star polymer arms are therefore most perturbed near the core and gradually obtains random coil conformation as it radiates outward; the arms can now be described as a succession of blobs $\xi(r)$ which increase in size with increasing distance from the core; i.e. the Daoud and Cotton star polymer model.
[28] Crassous J, Régisser R, Ballauf M, Willenbacher N. J Rheol 2005; 49(4):851–64.